# THE PERFORMANCE OF THE FOUNDATION UNDER A HIGH EMBANKMENT

by

T. William Lambe[1] – David J. D'Appolonia[2]
Kjell Karlsrud[3] – Robert C. Kirby[4]

## Abstract

This paper presents the measured performance of an embankment constructed on a deep deposit of soft clay. The most important aspect of this measured performance is the large differences in settlement among three closely spaced settlement platforms. Possible reasons for this difference are discussed. Predicted embankment performance is compared to the measured performance.

## I. Introduction

A one and a half mile section of Interstate Highway I-95 passes through a tidal marsh in the Revere-Saugus area north of Boston, Massachusetts. In 1957 a test embankment ("Northeast Test Embankment") was constructed along the then proposed route of a connector to I-95. The NE Test Embankment is close to an instrumented field test section ("MIT Test Section") constructed on the actual highway embankment. The performance of the MIT Test Section has been described (MIT, 1969, D'Appolonia et al, 1971, and Wolfskill and Soydemir, 1971). Figure 1 shows the locations of the NE Test Embankment and the MIT Test Section.

The soil in the area includes a thick layer of soft to medium clay, "Boston blue clay". The NE Test Embankment was constructed to obtain information needed for evaluating the stability of the embankments required for the highway extension. Settlement measurements were made during and after construction. A number of piezometers were installed in 1967, approximately ten years after construction.

This paper presents the measured performance of the NE Test Embankment. The most important aspect of this measured performance is the large

[1]T. William Lambe, Edmund K. Turner Professor of Civil Engineering, Massachusetts Institute of Technology.
[2]David J. D'Appolonia, Principal, Lambe Associates Inc.
[3]Kjell Karlsrud, Norwegian Geotechnical Institute.
[4]Robert C. Kirby, Research Assistant, Massachusetts Institute of Technology.

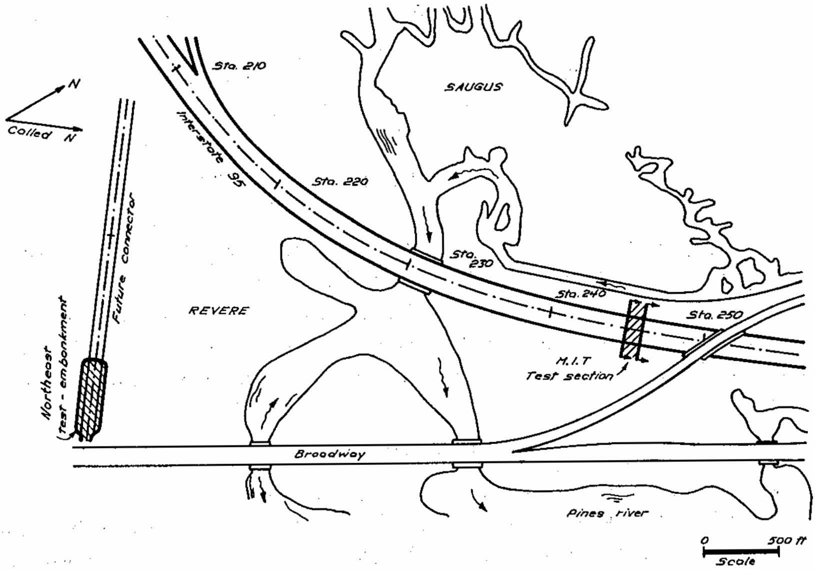


Figure 1. Location of Test Embankments

differences in settlement among three closely spaced settlement platforms. This paper discusses possible reasons for this difference and concludes that the information available is not sufficient to explain the observed performance. A typical section is chosen for analysis and the measured embankment performance compared to the predicted performance using several different analytical approaches. Comparisons are made between observed and predicted initial settlements, consolidation settlements, rates of consolidation settlement, and excess pore pressures. In each case the range of behaviors predicted by various methods, which range from simple to complex, is small relative to the differences in measured values. This fact suggests that the major portion of the engineering effort should be in exploration, testing and judgment.

## II. Soil Profile and Embankment Section

Figure 2 is a plan and section of the NE Test Embankment. The embankment crest is at El. +40 (El. 0 is mean sea level) and is 100 ft. wide and 400 ft. long. The side slopes are 1 vertical to 2 horizontal, with the exception of a truck ramp which has a slope of 1 to 10. The surrounding marsh is at El. +5. Figure 3 shows boring data.

The soil profile consists of silt, peat and sand, some or all of which were excavated prior to embankment construction, overlying a thin layer of stiff

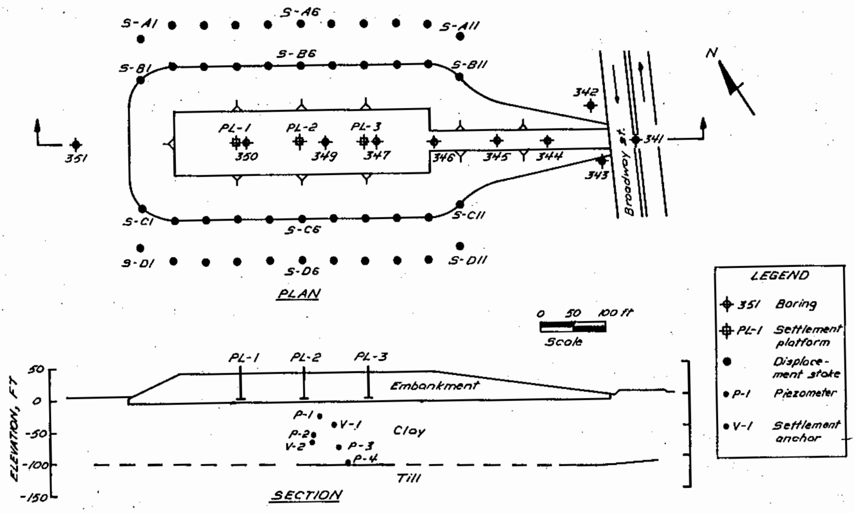


Figure 2. Northeast Test Embankment

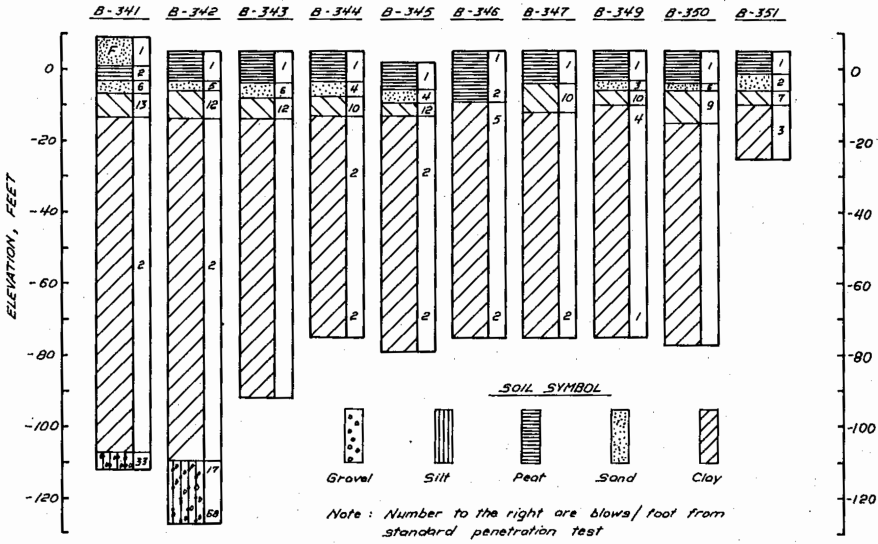


Figure 3. Boring Data

yellow clay which in turn overlies a thick layer of medium to soft Boston blue clay. The elevation of the bottom of the clay varies between El. -93 and El. -110. Above El. -70 the clay is overconsolidated, probably due to desiccation, and below El. -70 is normally consolidated. Results from laboratory tests are presented in a later section.

## III. Measured Embankment Performance

*A. Description of Field Instrumentation*

The embankment was instrumented in two stages. Prior to embankment construction, three settlement plates (PL-1, PL-2, PL-3) were installed at the base of the embankment and a network of surface displacement stakes placed along the toe of the embankment and 65 ft. from the toe. In 1967 four hydraulic peizometers (P-1 to P-4) and two settlement anchors (V-1, V-2) were installed. The instrument locations are shown in Fig. 2.

Each settlement plate (Fig. 4) consists of a four-foot square platform constructed of double planked 1-in. x 12-in. boards. Two 12-in. x 12-in. steel plates were bolted to the center of the platform and a threaded flange welded to the top plate. The platform was placed on granular backfill at El. +5 and a 2½-in. standard pipe attached to the platform and extended as necessary during construction. Level surveys were made to a plug at the top of the 2½-in. riser pipe.

The displacement stakes (Fig. 4) were 2-in. x 2-in. wooden posts driven to a depth of 5 ft. below the bottom of the peat and organic silt. Vertical and horizontal scales were attached to each stake and the movements were determined by optical surveys.

The hydraulic piezometers (Fig. 5) are Geonor A/S Model M-206 field piezometers. The piezometer consists of a hollow stem with a conical point at the bottom; three sintered bronze filters are mounted on the stem and separated by chamfered brass rings. The top of the hollow stem was attached to a drilling rod (E-rod) connector and sections of E-rod were then attached directly to the sensor. A single 3/8-in. plastic tube was used as a riser pipe. The piezometer was installed by first augering through the embankment fill into the medium clay, and then pushing the sensor by means of the attached E-rod to the final sensor elevation. The E-rod was left in place. The natural clay provided the piezometer seal.

The settlement anchors (Fig. 5), described as anchor posts, were manufactured by Borros (A/B. The anchor consists of two parts: the point and three anchor rods. The point is a 1¼-in. hollow steel cylinder with three circular milled grooves. A short section of 1-in. steel pipe is connected to the point and additional sections are added as necessary. The anchor rods are approximately 3/8-in. in diameter and are welded together at their upper ends and connected to

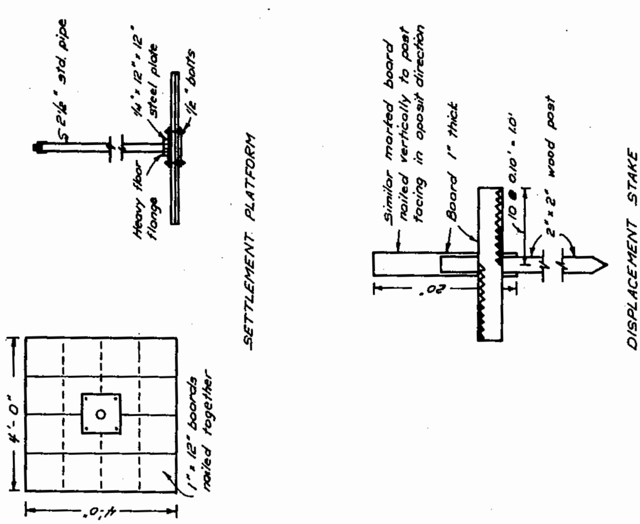


Figure 4. Instrument Details

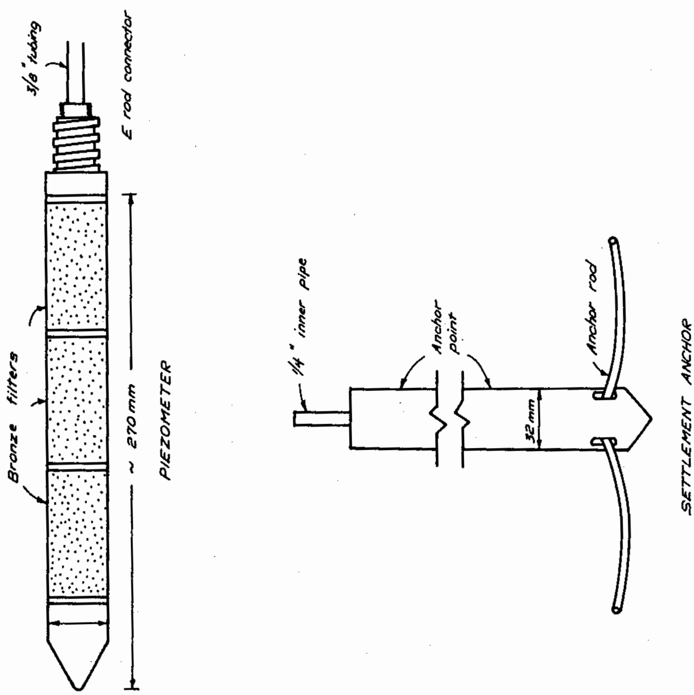


Figure 5. Instrument Details

a round plate. A short section of 1/4-in. steel pipe is then connected to the plate and additional sections added as necessary. The anchor was installed by first augering through the embankment fill and into the medium clay, then the assembled anchor is pushed to the proper elevation. The three anchor rods are extended by striking the 1/4-in. inner pipe forcing the three prongs out of the point. The 1-in. outer pipe is then disconnected at the point, by means of a left-hand threaded coupling at the point, and bumped back several feet. The 1-in. pipe now acts as a protective casing for the 1/4-in. pipe which is connected directly to the anchor. Level surveys are made to the top of the 1/4-in. pipe.

*B. Measured Field Performance*

Figure 6 shows settlement versus time for the three settlement plates and the two settlement anchors. Also shown are estimates of the settlement at the end of primary consolidation ($\rho_{TF}$), as obtained by Taylor's square root of time fitting method. There is an increasing spread among the measured settlements of the three plates and by the end of 1970 the measured settlements were 3.1 ft. at PL-1, 4.4 ft. at PL-2, and 5.7 ft. at PL-3. The reasons for these considerable differences in settlement are not clear. Possible reasons are given in the following section.

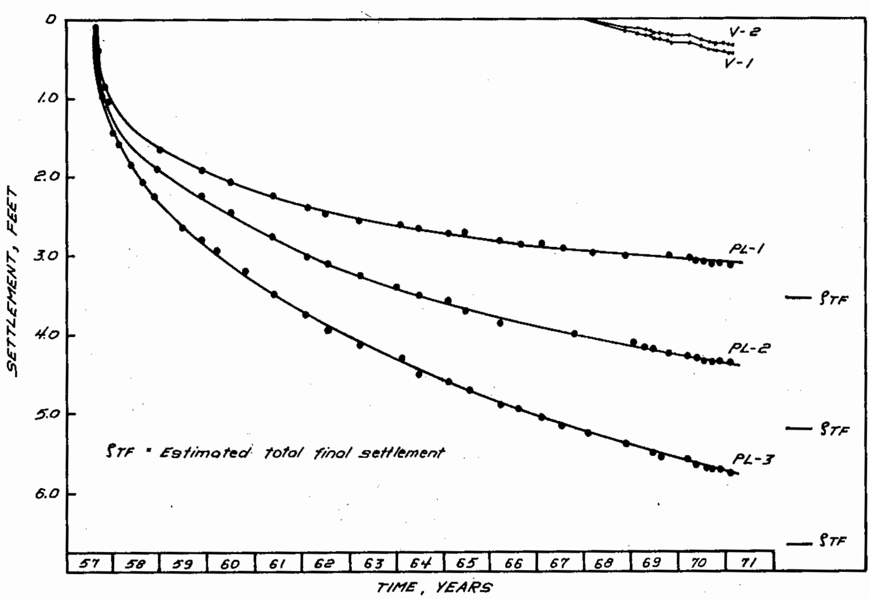


Figure 6. Embankment Settlement

The settlement anchors installed in 1967 show that the lower third of the clay layer is settling three times more than the middle third.

The displacement stakes were surveyed before construction and shortly after construction. The vertical movements observed are summarized in Table 1 and indicate a rotation of the embankment about its long axis. There is considerable scatter in the readings and the magnitude of movement being recorded (0.06 ft. maximum) is quite small compared to the probable accuracy of the survey (±.01 ft.).

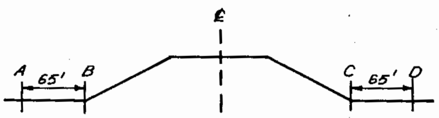


| Stake No. | Row A: 8/1/57 to 10/15/57 | Row A: 10/15/57 to 11/12/57 | Row A: Total | Row B: 8/1/57 to 10/15/57 | Row B: 10/15/57 to 11/12/57 | Row B: Total | Row C: 8/1/57 to 10/15/57 | Row C: 10/15/57 to 11/12/57 | Row C: Total | Row D: 8/1/57 to 10/15/57 | Row D: 10/15/57 to 11/12/57 | Row D: Total |
|---|---|---|---|---|---|---|---|---|---|---|---|---|
| 1 | +4 | -2 | +2 | -2 | +2 | 0 | +3 | -2 | +1 | -2 | 0 | -2 |
| 2 | -2 | -2 | -4 | -5 | +1 | -4 | +5 | -2 | +3 | -2 | +2 | 0 |
| 3 | -4 | -2 | -6 | -7 | +1 | -6 | +2 | -2 | 0 | -1 | +1 | 0 |
| 4 | -1 | -5 | -6 | -6 | -1 | -7 | +9 | -2 | +7 | -3 | 0 | -3 |
| 5 | +1 | -7 | -6 | -6 | 0 | -6 | +2 | -4 | -2 | -1 | 0 | -1 |
| 6 | +2 | -7 | -5 | -6 | -2 | -8 | +2 | -3 | -1 | 0 | -1 | -1 |
| 7 | +1 | -5 | -4 | -4 | -3 | -7 | -2 | -3 | -5 | +4 | -2 | +2 |
| 8 | 0 | -4 | -4 | -6 | -1 | -7 | +1 | -4 | -3 | +4 | -3 | +1 |
| 9 | +1 | -5 | -4 | -4 | -1 | -5 | +1 | -4 | -3 | 0 | - | - |
| 10 | +1 | -2 | -1 | -14 | -2 | -16 | -2 | -9 | -11 | -2 | -2 | -4 |
| 11 | +2 | -2 | 0 | -4 | -1 | -5 | +5 | - | - | -2 | -2 | -4 |

Note: (-) denotes upward movement, (+) downward
Movements are in hundredths of a foot

Table 1. Vertical Displacement Stake Movements
Northeast Test Embankment

Figure 7 indicates sizable excess pore pressures still remain in the clay ten years after construction. The measured pore pressures shown in Fig. 7 along with the predicted initial pore pressures indicate a degree of consolidation of 0.62 to 0.71.

## *C. Discussion*

The measured settlement versus time record (Fig. 6) at the three settlement plates is the most important aspect of the observed performance. There is an increasing spread among the settlements of the three plates. Calculations indicate that this spread cannot be attributed to the differences in location of the plates.

An initial question is: Do the data reflect the actual performance of the clay foundation? The construction of the settlement platforms has already been described and is similar to that of the settlement plates in common use today.

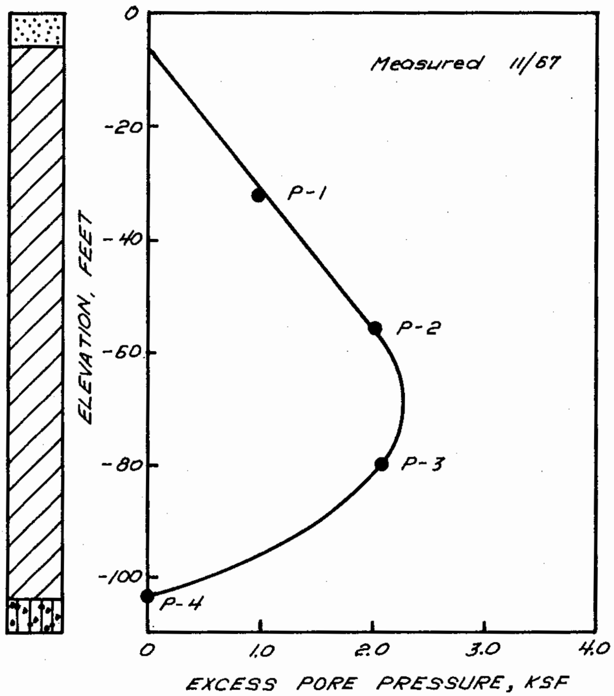


Figure 7. Excess Pore Pressure 10 Years After Construction

The main flaw in this instrument is the possible interaction between the embankment fill and the pipe extending from the platform at the base of the embankment to the embankment crest. As the embankment itself compresses due to additional lifts of the fill, the friction between the fill and the pipe tends to drag the pipe down. Embankment arching due to settlement of the foundation could cause the opposite effect, holding the pipe up. The effects of this interaction are thought to be too small to explain the observed differences in the settlements of the three plates.

The proper installation of the platforms is very important. The peat and organic silt which initially covered the site were excavated under water and then the area backfilled with granular material. Before backfilling a survey was made to determine the depth of excavation. The possibility exists that some of the peat was not excavated. After backfilling with sand to the elevation of the settlement platform (El. +5), the presence of a local pocket of peat would go unnoticed, but would clearly influence how much the platform would settle under the embankment loading.

Survey errors should also be considered. The bench mark used, a disk set by the U.S. Coast and Geodetic Survey, is located in the median strip of

Broadway Street which is adjacent to the test embankment. Both changes in the elevation of the bench mark and survey errors are possible but cannot explain the differences in movements of the three plates.

Of the three possible sources of error in measuring the settlement, the existence of a local pocket or layer of peat and organic silt is the only one that could lead to the large differences in settlements observed. If a pocket of peat were present under a platform, one would expect the peat to compress quite rapidly because of its relatively high permeability and the closeness of a drainage layer. The measured settlements are nearly identical during the loading period and the differences in settlement steadily increase with time. This observed performance does not support the hypothesis of pockets of peat under the settlement platforms. Also, the construction record indicates that reasonable care was taken to ensure that the peat and silt were removed. It is concluded that there is little reason to suspect the validity of the field measurements.

The observed behavior must be due to variations in thickness or compressibility and consolidation characteristics of the soil beneath the embankment. Figure 8 summarizes oedometer data on undisturbed samples of Boston blue clay from the I-95 site and the M.I.T. campus. The clay is overconsolidated, probably due to desiccation, above El. -70 and normally consolidated below. Figure 9 summarizes the results of special stress path triaxial tests performed on undisturbed samples obtained 250 ft. from the center line of the NE Test Embankment. The stress path method, as outlined by Lambe (1964), had to be modified to take into account local yielding of the clay during undrained loading. The modified test procedure consisted of reconsolidating the sample to the estimated in situ stresses and then applying only a portion of the change in stress due to the embankment loading and calculating pseudo-elastic constants. Figure 10 shows the coefficient of volume change, $m_v$, and coefficient of consolidation, $c_v$, determined from the oedometer data and the stress path triaxial data. The agreement is quite good and increases our confidence in both sets of data. No distinct variation in soil properties can be recognized from the laboratory data.

The borings made in the vicinity of the NE Test Embankment are shown in Fig. 3. The limited blow count data do not indicate a variation in foundation properties along the axis of the embankment.

Another indication of the nature of the compressibility and consolidation characteristics of the clay is provided by settlement measurements along the main embankment of the I-95 extension. Settlement platforms were installed at the base of the embankment about 100 ft. apart all along the main embankment which was completed in 1968. Settlement data between Station 225 and Station 265 (see Fig. 1) are summarized in Fig. 11. These measurements were made 20 months after construction. Between Station 237 and Station 255 the embankment crest elevation is +40 and the thickness of the compressible soil is

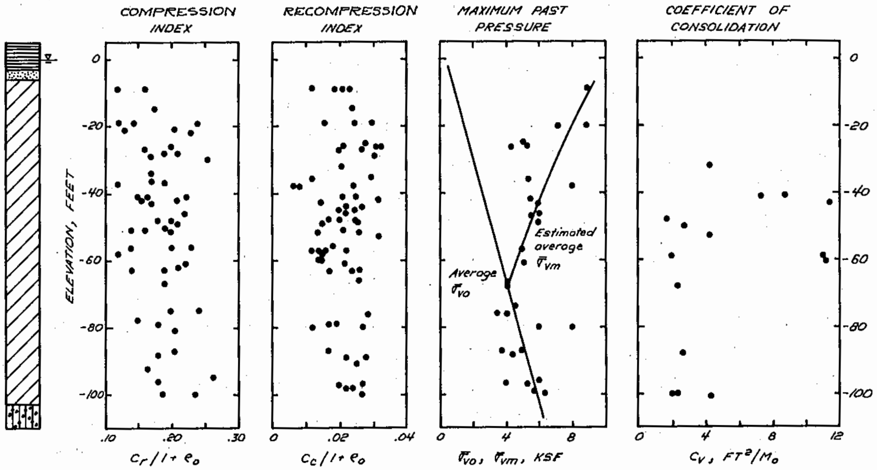


Figure 8. Summary of Oedometer Data

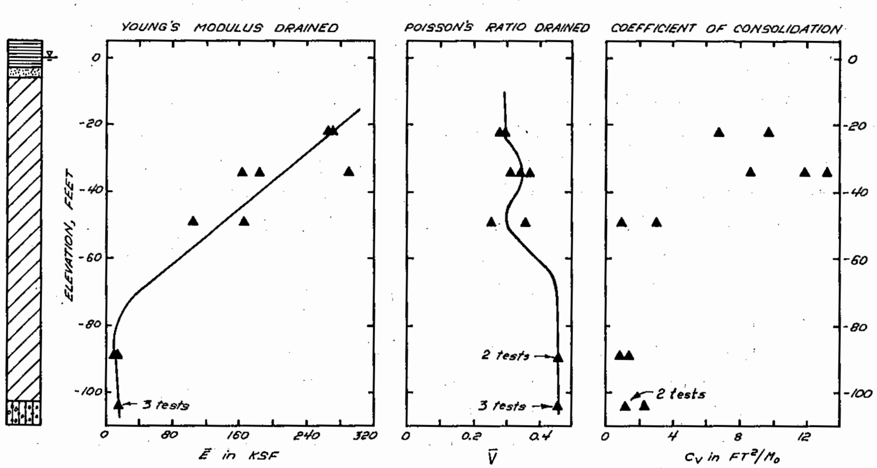


Figure 9. Summary of Stress Path Triaxial Data

approximately constant. The measured settlements in this area are very nearly the same. This fact indicates that the clay along this 1800-ft. stretch of embankment has the same compressibility and consolidation properties.

The reasons for the increase in settlement near Station 260, where the thickness of the clay decreases rapidly, are not clear. The total final settlement

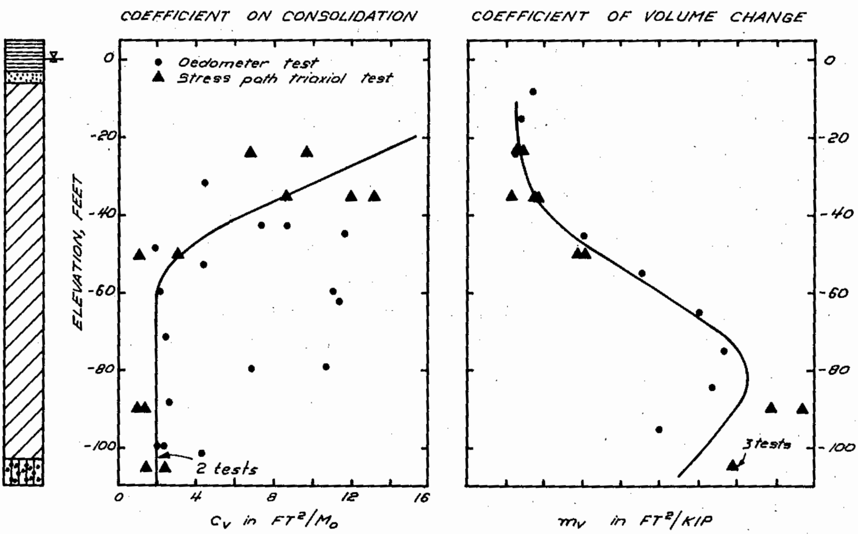


Figure 10. Comparison of Oedometer and Stress Path Data

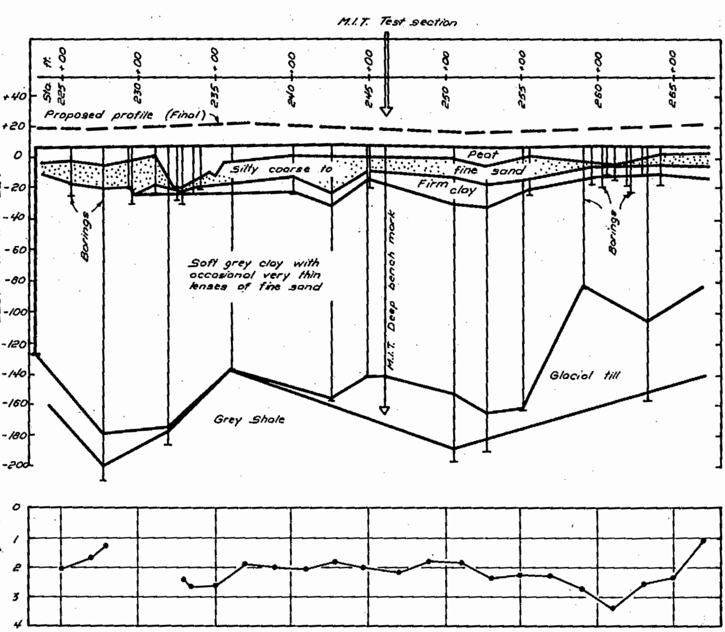


Figure 11. Measured Settlement Along Main Embankment
20 Months After Construction

of the shallow deposit should be less than that of the deeper deposit. However, the decrease in length of drainage path and the increase in average $c_v$ for the shallow clay layer would accelerate the rate of consolidation markedly when compared to the rate of the adjacent thicker clay layer. It is then possible for the settlement of the shallow deposit to be equal to or greater than the settlement of the thicker deposit at early times. This explanation is by no means completely satisfactory, but should point out that other factors besides variation in soil properties can be cited to explain this seemingly anomalous behavior.

Therefore, all the available laboratory and boring data, as well as field measurements on the nearby main embankment, indicate that the variation in soil properties over the site is small. The next factor to consider is the effect of variation in thickness of the clay layer.

An example of the effect of variation of thickness of the clay has already been discussed. At Station 260 along the main embankment the variation in soil thickness has been cited as one factor causing the marked change in behavior. The effect of the thickness of the clay has also been investigated analytically. Settlement calculations for embankments on 80, 100, and 120 feet of clay indicate a range of settlements from 3.0 to 5.7 feet. Clearly, the thickness of compressible soil is an important factor and Fig. 3 shows that the thickness of clay in the area of the NE Test Embankment has only been determined at three points. There are not enough deep borings to adequately define the thickness of compressible soil beneath the NE Test Embankment and a variation in thickness could account for the observed performance.

## IV. Comparison between Predicted and Observed Performance

Since the observed embankment performance cannot be explained with the information available from the exploration and testing program, it is clear that the observed performance could not have been correctly predicted. Nevertheless, a complete analysis of a representative section, using several analytical methods and soil properties determined from different laboratory tests, will provide a means of evaluating the importance of the method of analysis and laboratory testing procedures when predicting performance.

### *A. Embankment Section and Soil Properties*

The section chosen for analysis is shown in Fig. 12. The thickness of the clay layer was taken as that at the location of piezometer P-4. A plane strain condition was assumed.

The results of oedometer tests and special stress path triaxial tests have already been presented (Figs. 8, 9, 10). Values of undrained modulus, determined from U and UU tests, special stress path triaxial tests, and an

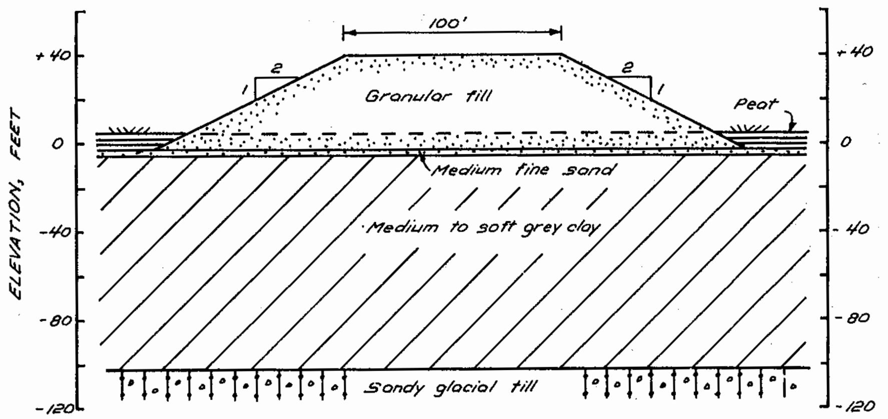


Figure 12. Section Chosen for Analysis

empirical correlation suggested by D'Appolonia, et al (1970), are presented in Fig. 13. The shear strength of the soil was determined from U and UU tests and $CK_0U$ triaxial compression tests. The data are summarized in Fig. 14.

*B. Initial Settlement*

Four analytical methods used for predicting initial settlement are summarized in Table 2. The first two methods make direct use of elastic theory. Skempton and Bjerrum's method requires that a single value of modulus be used, while the elastic strain summation method suggested by Davis and Poulos (1968) takes into account the variation of modulus with depth. The modified elastic displacement method was proposed by D'Appolonia, et al (1970) as a means of taking into account the effects of local yielding. A correction factor based on theoretical considerations is used to correct the computed elastic displacement. The finite element method described by D'Appolonia and Lambe (1970) takes into account variation of modulus with depth and local yielding.

Table 3 presents the results of the four analyses, each using values of undrained modulus determined by three different methods (Fig. 13). The predicted initial settlements vary from 0.1 ft. to 0.6 ft. and are more sensitive to the modulus than the method of analysis. The actual initial settlement was estimated by reducing the observed settlement at the end of the loading period by an estimate of the amount of consolidation settlement that took place during loading. The initial settlement of all three plates was found to be 0.5 feet. The

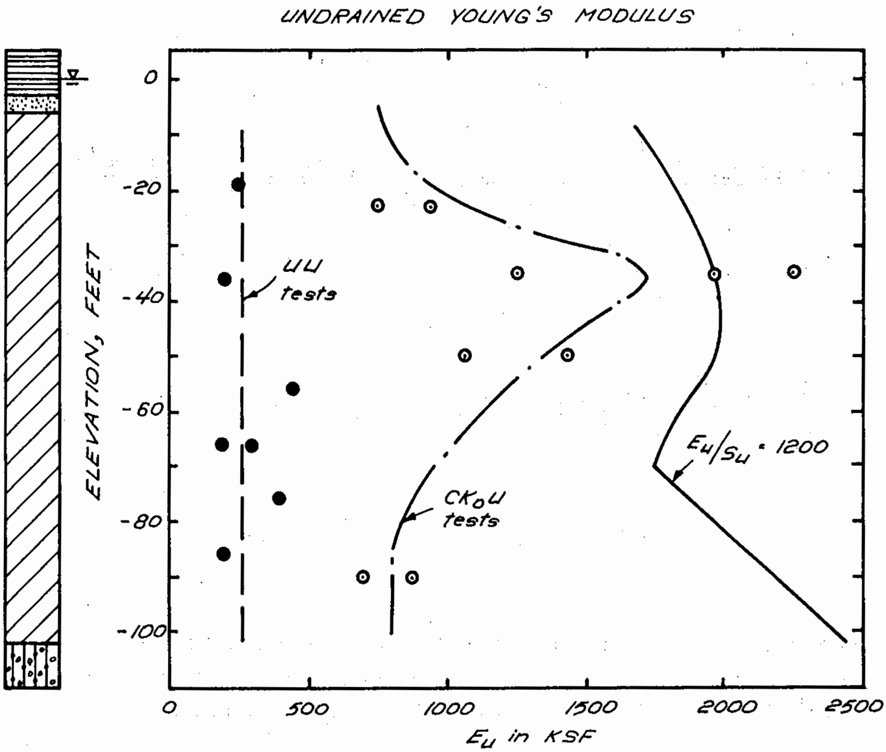


Figure 13. Undrained Modulus

elastic displacement method using modulus determined from U and UU tests provided the best estimate of the initial settlement.

## *C. Total Final Settlement*

Table 4 summarizes five methods of predicting total final settlement which is defined as initial settlement plus consolidation settlement. The first two methods assume that one-dimensional strain occurs during the consolidation process and the initial settlement is added to the consolidation settlement to give the total final settlement. The last three methods predict directly the total final settlement based on three-dimensional strain and pseudoelastic parameters of the soil skeleton.

| METHOD | FORMULA | REFERENCE |
|---|---|---|
| 1. Elastic displacement | $\rho_i = \frac{qBI}{E_u}$ | Skempton & Bjerrum (1957) |
| 2. Elastic strain summation | $\rho_i = \sum\left[\frac{\sigma_z - 1/2(\sigma_x + \sigma_y)}{E_u}\right]\Delta z$ | Davis & Poulos (1968) |
| 3. Modified elastic displacement | $\rho_i = S_R\left[\frac{qBI}{E_u}\right]$ | D'Appolonia et al (1970) |
| 4. Finite element | By computer ($E_u$, $S_u$, $\sigma_{vo}$, $\sigma_{ho}$) | D'Appolonia & Lambe (1970) |

Table 2 Methods of Predicting Initial Settlement

| METHOD | PREDICTED INITIAL SETTLEMENT, FT | | |
|---|---|---|---|
| | $E_u$ from UU tests | $E_u$ from $CK_oU$ tests | $E_u$ from $E_u/S_u = 1200$ |
| 1. Elastic displacement | 0.61 | 0.15 | 0.09 |
| 2. Elastic strain summation | 0.61 | 0.13 | 0.08 |
| 3. Modified elastic displacement | Failure | 0.22 | 0.12 |
| 4. Finite element | Failure | 0.21 | 0.11 |

Table 3 Predicted Initial Settlement

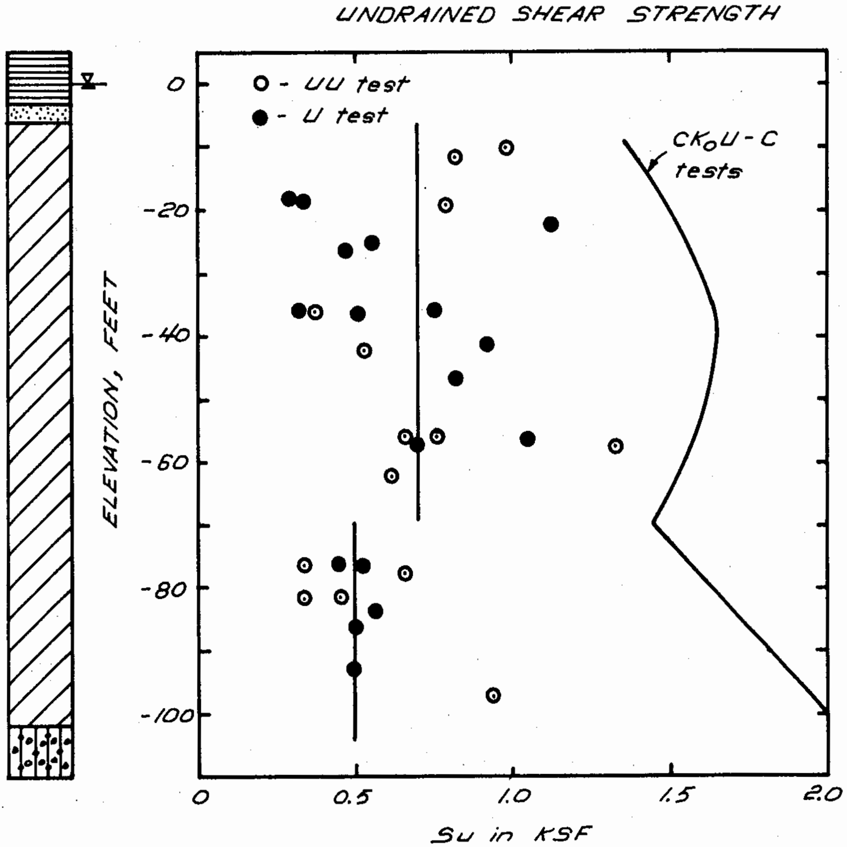


Figure 14. Undrained Shear Strength

Predictions were made using data from oedometer tests and special stress path triaxial tests. Table 5 summarizes the results of these predictions and Fig. 15 compares the measured and the predicted performances. The predicted total final settlements range from 2.2 to 4.4 feet. The elastic displacement method gives the lowest predicted settlement and this is due to the large variation of modulus with depth which cannot be modeled using an average value. Discounting the elastic displacement analysis, the predicted settlements range from 3.4 to 4.4 feet. The predictions were relatively insensitive to the method of analysis and the type of laboratory test used to determine the soil parameters. Both these observations are not surprising since it has already been shown that the data from the oedometer tests and special triaxial tests are in good

| METHOD | FORMULA | REFERENCE |
|---|---|---|
| 1. One dimensional | $\rho_{TF} = \rho_i + \rho_{oed}$ | Terzaghi (1943) |
| 2. Skempton - Bjerrum | $\rho_{TF} = \rho_i + u\,\rho_{oed}$ | Skempton & Bjerrum (1957) |
| 3. Elastic displacement | $\rho_{TF} = \frac{qB\,I(1-\nu)^2}{\bar{E}}$ | Davis & Poulos (1968) |
| 4. Elastic strain summation | $\rho_{TF} = \sum\left[\frac{\bar{\sigma}_z - \bar{\nu}(\bar{\sigma}_x + \bar{\sigma}_y)}{\bar{E}}\right]\Delta z$ | Davis & Poulos (1968) |
| 5. Finite element | By computer $(\bar{E}, \nu)$ | |

Table 4 Methods of Predicting Total Final Settlement

| METHOD | PREDICTED TOTAL FINAL SETTLEMENT FEET | | | |
|---|---|---|---|---|
| | OEDOMETER DATA | | | $\bar{E}, \bar{\nu}$ from stress path triaxial tests |
| 1. One dimensional | 4.10 | | | - |
| 2. Skempton - Bjerrum | 3.38 | 3.55 | 3.92 | - |
| 3. Elastic displacement | 2.90 | | | 2.19 |
| 4. Elastic strain summation | 4.31 | | | 4.23 |
| 5. Finite element | 4.36 | | | 4.33 |

Table 5 Predicted Total Final Settlement

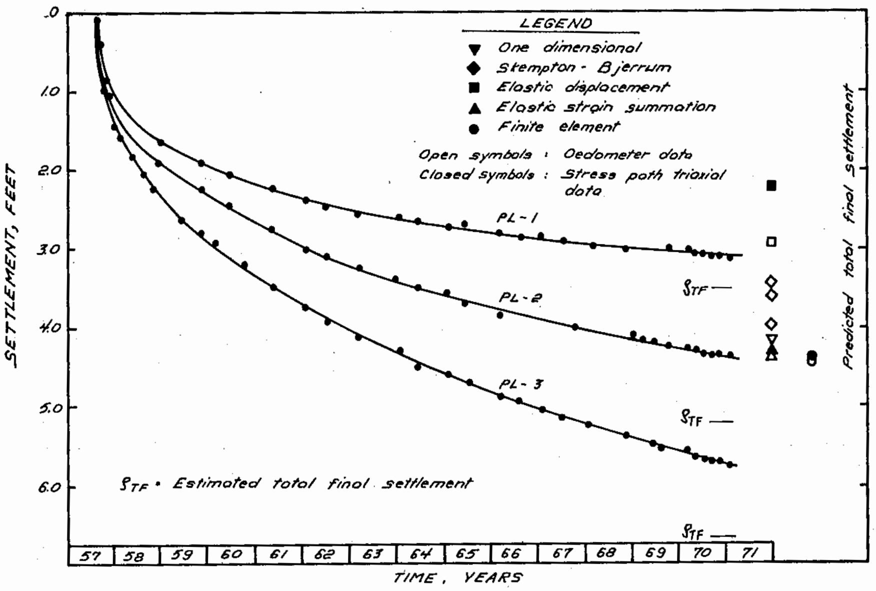


Figure 15. Comparison of Measured and Predicted Total Final Settlement

agreement (Fig. 10), and the geometry of the section being analyzed is such that lateral strains are not very important. One-dimensional analysis should work well on a one-dimensional problem and the general three-dimensional approach should work on a one-dimensional problem.

## D. *Rate of Settlement*

A rational approach to predicting the rate of settlement involves using theoretical solutions based on the strain and drainage conditions which are present in the problem being analyzed. The analysis of total final settlement made above has shown that, for the geometry of the section being studied, considering only vertical strain is a good approximation to the more exact three-dimensional analysis. Therefore, theoretical solutions based on one-dimensional strain should give a good prediction of the rate of settlement. The drainage conditions, whether one, two or three-dimensional, must also be specified. Theoretical solutions by Davis (1969) indicate that one-dimensional drainage is also a reasonable approximation provided the vertical and horizontal permeabilities of the soil are the same. Davis also notes that anisotropic permeability has an important effect and presents correction factors, based on theoretical studies, to account for this.

Table 6 summarizes the methods used to predict the rate of settlement. The first two methods assume one-dimensional strain and drainage, whereas the third takes into account two-dimensional drainage due to anisotropic permeability. Oedometer tests were run on two samples cut from the same undisturbed soil sample. One sample was trimmed and tested in the usual way and the other cut vertically from the undisturbed sample and tested. The coefficient of consolidation was found to be eight times larger for the sample cut vertically than the sample cut in the usual manner.

Figure 16 compares our best estimate of the rates of settlement of the three settlement plates to the rates predicted by the three analytical methods. The approximate nature of the estimated rate of consolidation settlement of the three settlement plates should be recognized. The consolidation settlement was estimated by subtracting the estimated initial settlement from the estimated total final settlement. The degree of consolidation at any time was then computed as the ratio of the measured total settlement minus the estimated initial settlement divided by the estimated consolidation settlement.

The comparison shows that all the predicted rates are too slow. However,

| METHOD | REFERENCE |
|---|---|
| 1. 1-D Strain and drainage average $m_v$ and $C_v$ | Terzaghi (1943) |
| 2. 1-D Strain and drainage distribution of $m_v$ and $C_v$ | Schiffman and Gibson (1967) |
| 3. 1-D Strain and 2-D drainage distribution of $m_v$ and $C_v$ | Davis (1969) |

Table 6. Methods of Predicting Rate of Settlement

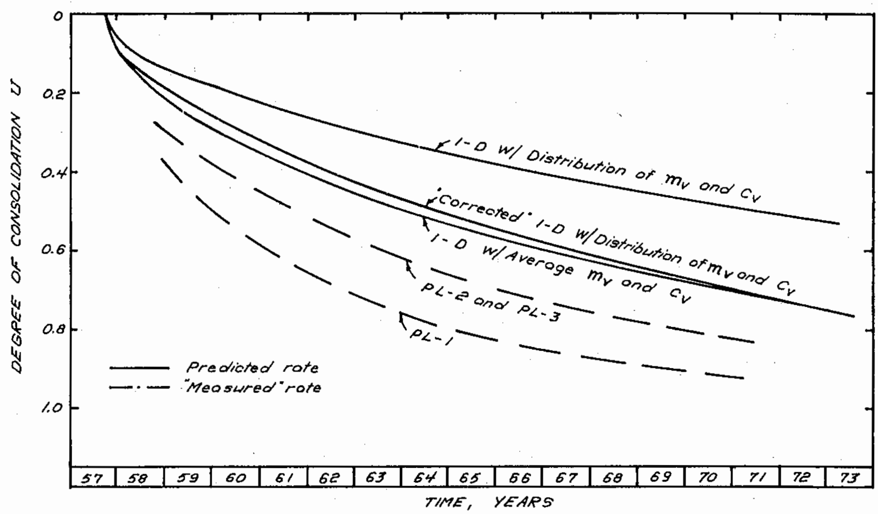


Figure 16. Comparison of "Measured" and Predicted Rates of Settlement

the analysis demonstrates two well-known facts, 1) using an average $c_V$ and $m_V$ is not a good approximation when $c_V$ and $m_V$ vary with depth, and 2) anisotropic permeability should be considered in any rate of settlement calculation. The close agreement between the analysis assuming one-dimensional strain and drainage with constant $m_V$ and $c_V$ with depth and the analysis assuming one-dimensional strain and two-dimensional drainage with $m_V$ and $c_V$ varying with depth must be considered fortuitous.

Figure 17 is a comparison between the measured excess pore pressure ten years after construction and that predicted by the three analytical methods. The close agreement using the third method is encouraging, but the failure of this method to predict the rate of settlement should be noted.

## V. Summary and Conclusions

This study of the NE Test Embankment yields two important results:

1. The available data from the exploration and field testing program are not sufficient to explain the observed behavior.
2. The differences in the performances predicted by several methods of analysis are small compared to the differences in measured performances.

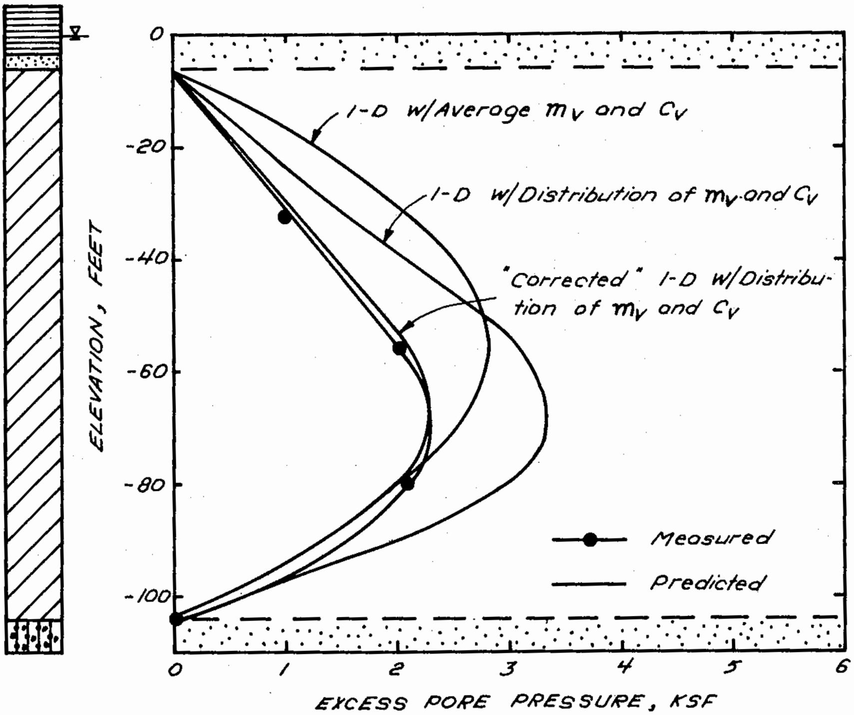


Figure 17. Comparison of Measured and Predicted Excess Pore Pressure 10 Years After Construction

These results suggest that the following recommendations should be considered when attempting to predict the performance of an embankment on soft soil:

1. The major engineering effort should be in field exploration and testing combined with sound engineering judgment. The key to predicting performance is a knowledge of boundary conditions and soil properties. Our most sophisticated analytical tools are no better than the input data.

2. Predicted performance should be checked by field measurements and these field measurements should be checked. The importance of having three settlement plates on the NE Test Embankment is an example. If only one settlement plate were installed the tilting of the embankment would have gone unnoticed.

## VI. Acknowledgements

The research described in this paper was supported by the Department of Public Works, Commonwealth of Massachusetts, and the Bureau of Public Roads, U. S. Department of Transportation. The authors appreciate the support they have received from the sponsors, especially Mr. John J. Lyons, Research and Materials Engineer, Mr. Paul McHugh, Assistant Research and Materials Engineer, Mr. Robert T. Tierney, Deputy Chief Engineer for Highway Maintenance, and Mr. Charles Whitcomb, Deputy Chief Engineer for Highway Design, all of the Massachusetts Department of Public Works.

Many people from the M.I.T. Department of Civil Engineering participated in the research. The field work was done under the direction of Dr. L.A. Wolfskill. Dr. C. Soydemir and Mr. W.R. Beckett have participated in field supervision and data processing.

Dr. Harry G. Poulos, Senior Lecturer, Department of Civil Engineering, University of Sydney, carried out preliminary analytical studies while a Visiting Lecturer at M.I.T.

The opinions, findings and conclusions expressed in this publication are those of the authors and not necessarily those of the Massachusetts Department of Public Works or the Bureau of Public Roads.

## Appendix I – References

D'Appolonia, D.J. and T.W. Lambe, "A Method for Predicting Initial Settlement", ASCE, Journal of the Soil Mechanics and Foundations Division, SM2, March 1970.

D'Appolonia, D.J., H.G. Poulos and C.C. Ladd, "Initial Settlement of Structures on Clay", ASCE Journal of Soil Mechanics and Foundation Division, Vol. 97, SM10, October 1971.

D'Appolonia, D.J., T.W. Lambe and H.G. Poulos, "Evaluation of Pore Pressures Beneath an Embankment", ASCE, Journal of the Soil Mechanics and Foundation Division, Vol. 97, SM6, June 1971.

Davis, E.H., "Rate of Settlement", Lectures 3 and 4 of a course entitled *The Analysis of the Settlement of Foundations,* University of Sydney, June-July 1969.

Davis, E.H. and H.G. Poulos, "The Use of Elastic Theory for Settlement Prediction Under Three-Dimensional Conditions", Geotechnique, Vol. XVIII, No. 1, March 1968.

Lambe, T.W., "Methods of Estimating Settlement", ASCE, Journal of the Soil Mechanics and Foundations Division, SM2, September 1964.

MIT, "Performance of an Embankment on Clay Interstate-95, Department of Civil Engineering, Research Report R69-67", Massachusetts Institute of Technology, Cambridge, Massachusetts, October 1969.

Schiffman, R.L. and R.E. Gibson, "Consolidation of Non-Homogeneous Clay Layers", ASCE, Journal of the Soil Mechanics and Foundation Division, SM5, 1964.

Skempton, A.W. and L. Bjerrum, "A Contribution to the Settlement Analysis of Foundations on Clay", Geotechnique, Vol. VII, 1957.

Terzaghi, K., *Theoretical Soil Mechanics,* John Wiley and Sons, New York, 1943.

Wolfskill, L.A. and C. Soydemir, "Soil Instrumentation for the I-95 MIT–MDPW Test Embankment", BSCE Journal, Vol. 58, October 1971.

## Appendix II – Notation

The following symbols are used in this paper:

| | | |
|---|---|---|
| $B$ | = | foundation width |
| $C_c$ | = | compression index |
| $C_r$ | = | recompression index |
| $c_v$ | = | coefficient of consolidation |
| $\overline{E}$ | = | Young's modulus for drained loading |
| $E_u$ | = | Young's modulus for undrained loading |
| $e_o$ | = | initial void ratio |
| $I$ | = | displacement influence factor |
| $K_o$ | = | coefficient of lateral earth stress at rest |
| $m_v$ | = | coefficient of volume change |
| $q$ | = | applied foundation stress |
| $S_R$ | = | Correction factor to account for local yield |
| $s_u$ | = | undrained shear strength |
| $\Delta\sigma_x, \Delta\sigma_y, \Delta\sigma_z$ | = | change in total stress in x, y, and z directions |
| $\Delta\overline{\sigma}_x, \Delta\overline{\sigma}_y, \Delta\overline{\sigma}_z$ | = | change in effective stress in x, y, and z directions |
| $\mu$ | = | correction factor to account for initial settlement |
| $\nu$ | = | Poisson's ratio for undrained loading |
| $\overline{\nu}$ | = | Poisson's ratio for drained loading |
| $\rho_i$ | = | initial settlement |
| $\rho_{oed}$ | = | settlement assuming one-dimensional direction |
| $\rho_{TF}$ | = | total final settlement |
| $\overline{\sigma}_{vo}$ | = | initial effective vertical stress |
| $\overline{\sigma}_{ho}$ | = | initial effective horizontal stress |
| $\overline{\sigma}_{vm}$ | = | maximum past vertical consolidation stress |
| $CK_oU\text{–}C$ | = | consolidated undrained triaxial compression test when sample is consolidated in $K_o$ condition |
| U | = | unconfined compression test |
| UU | = | unconsolidated-undrained compression test. |